

# Lawrence Berkeley National Laboratory

## Lawrence Berkeley National Laboratory

### **Title**

Genome analysis of *Elusimicrobium minutum*, the first cultivated representative of the Elusimicrobia phylum (formerly Termite Group 1)

### **Permalink**

<https://escholarship.org/uc/item/971192v5>

### **Author**

Herlemann, D. P. R.

### **Publication Date**

2009-08-25

**Genome analysis of *Elusimicrobium minutum*, the first cultivated representative of the *Elusimicrobia* phylum (formerly Termite Group 1)**

D. P. R. Herlemann<sup>1</sup>, O. Geissinger<sup>1</sup>, W. Ikeda-Ohtsubo<sup>1</sup>, V. Kunin<sup>2</sup>,  
H. Sun<sup>2</sup>, A. Lapidus<sup>2</sup>, P. Hugenholtz<sup>2</sup> and A. Brune<sup>1\*</sup>

<sup>1</sup> *Max Planck Institute for Terrestrial Microbiology, Karl-von-Frisch-Strasse,  
35043 Marburg, Germany*

<sup>2</sup> *US DOE Joint Genome Institute, 2800 Mitchell Drive B100,  
Walnut Creek, CA 94598-1698, USA*

Running title:

Genome analysis of *Elusimicrobium minutum*

\* Corresponding author: Max Planck Institute for Terrestrial Microbiology, Karl-von-Frisch-Strasse, 35043 Marburg, Germany. Phone: +49-6421-178701, Fax: +49-6421-178709. E-mail: [brune@mpi-marburg.mpg.de](mailto:brune@mpi-marburg.mpg.de)

## Abstract

1 The candidate phylum Termite group 1 (TG1), is regularly encountered in termite hindguts but  
2 is present also in many other habitats. Here we report the complete genome sequence (1.64  
3 Mbp) of *Elusimicrobium minutum* strain Pei191<sup>T</sup>, the first cultured representative of the TG1  
4 phylum. We reconstructed the metabolism of this strictly anaerobic bacterium isolated from a  
5 beetle larva gut and discuss the findings in light of physiological data. *E. minutum* has all  
6 genes required for uptake and fermentation of sugars via the Embden-Meyerhof pathway,  
7 including several hydrogenases, and an unusual peptide degradation pathway comprising  
8 transamination reactions and leading to the formation of alanine, which is excreted in  
9 substantial amounts. The presence of genes encoding lipopolysaccharide biosynthesis and the  
10 presence of a pathway for peptidoglycan formation are consistent with ultrastructural evidence  
11 of a Gram-negative cell envelope. Even though electron micrographs showed no cell  
12 appendages, the genome encodes many genes putatively involved in pilus assembly. We  
13 assigned some to a type II secretion system, but the function of 60 *pilE*-like genes remains  
14 unknown. Numerous genes with hypothetical functions, e.g., polyketide synthesis, non-  
15 ribosomal peptide synthesis, antibiotic transport, and oxygen stress protection, indicate the  
16 presence of hitherto undiscovered physiological traits. Comparative analysis of 22  
17 concatenated single-copy marker genes corroborated the status of *Elusimicrobia* (formerly  
18 TG1) as a separate phylum in the bacterial domain, which was so far based only on 16S rRNA  
19 sequence analysis.

## Introduction

20 At least half of the phylum-level lineages within the domain *Bacteria* do not comprise pure  
21 cultures, but are rather represented only by 16S rRNA gene sequences of environmental origin  
22 (43). The number of such "candidate phyla" is still growing, and the biology of the members  
23 of these phyla is usually completely obscure. The first sequences of the candidate phylum  
24 Termite Group 1 (TG1; 23) were obtained from the hindgut of the termite *Reticulitermes*  
25 *speratus*, where they represent a substantial portion of the gut microbiota (21, 41).  
26 Meanwhile, numerous sequences affiliated with this phylum have been retrieved also from  
27 habitats other than termite guts. They form several deep-branching lineages comprising  
28 sequences derived not only from intestinal tracts but also from soils, sediments, and  
29 contaminated aquifers (14, 20).

30 Recently, we were able to isolate strain Pei191<sup>T</sup>, the first pure-culture representative of the  
31 TG1 phylum, from the gut of a humivorous scarab beetle larva, *Pachnoda ephippiata* (14).  
32 Based on the 16S rRNA gene sequence, strain Pei191<sup>T</sup> is a member of the "Intestinal cluster",  
33 which consists of sequences derived from invertebrate guts and cow rumen (20) and is only  
34 distantly related to the Endomicrobia, a lineage of TG1 bacteria comprising endosymbionts of  
35 termite gut protozoa (24, 42, 54). It is an obligately anaerobic ultramicrobacterium that grows  
36 heterotrophically on glucose and produces acetate, hydrogen, ethanol, and alanine as major  
37 products (14). The species description of *Elusimicrobium minutum*, with strain Pei191<sup>T</sup> as the  
38 type strain, and the proposal of *Elusimicrobia* as the new phylum name are published in a  
39 companion paper (14).

40 Here, we report the complete genome sequence of *E. minutum*, focusing on a reconstruction of  
41 the metabolism of this strictly anaerobic bacterium. The implications of these findings are

42 discussed in light of physiological data, and potential functions indicated by the genome  
43 annotation are compared to requirements imposed by the intestinal environment. Using the  
44 concatenated sequences of 22 single-copy marker genes of *E. minutum* and of the uncultivated  
45 "*Endomicrobium*" strain Rs-D17, an endosymbiont of termite gut flagellates (22), we also  
46 investigated the phylogenetic position of *Elusimicrobia* relative to other bacterial phyla.

## Material and Methods

47 **DNA preparation.** A 400-ml culture of *Elusimicrobium minutum* strain Pei191<sup>T</sup> grown on  
48 glucose (14) was harvested by centrifugation. Cells were resuspended in 500 µl TE buffer (10  
49 mM Tris-HCl, 1 mM EDTA, pH 8.0), and 30 µl of 10% SDS and 3 µl of proteinase K (20  
50 mg/ml) were added. The mixture was incubated at 37 °C for 1 h. The lysate was extracted  
51 three times with an equal volume of phenol-chloroform-isoamyl alcohol (49:49:1, by vol)  
52 using Phase Lock Gel tubes (Eppendorf). The supernatant was transferred to a fresh tube, and  
53 the DNA was precipitated with 0.6 volumes of isopropanol, washed with ice-cold 80%  
54 (vol/vol) ethanol, and air-dried. Quality and quantity were checked by agarose gel  
55 electrophoresis.

56 **Genome sequencing, assembly, and gap closure.** The genome of *E. minutum* was sequenced  
57 at the Joint Genome Institute (JGI) using a combination of 8-kb and 40-kb Sanger libraries  
58 and 454 pyrosequencing. All general aspects of library construction and sequencing performed  
59 at the JGI can be found at <http://www.jgi.doe.gov/>. 454 pyrosequencing reads were assembled  
60 using the Newbler assembler (Roche). Large Newbler contigs were chopped into 1871  
61 overlapping fragments of 1000 bp and entered into the assembly as pseudo-reads. The

62 sequences were assigned quality scores based on Newbler consensus q-scores with  
63 modifications to account for overlap redundancy and adjust inflated q-scores. A hybrid  
64 assembly of 454 and Sanger reads was performed using the PGA assembler. Possible mis-  
65 assemblies were corrected and gaps between contigs were closed by custom primer walks  
66 from sub-clones or PCR products. The error rate of the completed genome sequence of *E.*  
67 *minutum* is less than 1 in 50,000. The complete nucleotide sequence and annotation of *E.*  
68 *minutum* has been deposited at GenBank under accession number CP001055.

69 **Annotation.** Sequences were automatically annotated at the Oak Ridge National Laboratory  
70 (ORNL) according to the genome analysis pipeline described in Hauser et al. (18). All  
71 automatic annotations with functional prediction were also checked manually with the  
72 annotation platform provided by Integrated Microbial Genomes (IMG) (37). For each gene,  
73 the specific functional assignments suggested by the matches with the NCBI non-redundant  
74 database were compared to the domain-based assignments supplied by the  
75 COG/PFAM/TIGRFAM/INTERPRO databases, and if necessary corrected accordingly. When  
76 it was not possible to infer function or COG domain membership (RPS BLAST against COG  
77 PSSM with e-value  $> 10^{-2}$ ), genes were annotated as predicted to be novel. For all the genes,  
78 the subcellular location of their potential gene products was determined based on the presence  
79 of transmembrane helices and signal peptides. Putative transport proteins were compared to  
80 those in the Transport Classification Database (<http://www.tcdb.org>). Genes were viewed  
81 graphically with Integrated Microbial Genomes. Metabolic pathways were reconstructed using  
82 MetaCyc as a reference data set (7). Detailed information about the automatic genome  
83 annotation can be obtained from the JGI IMG website  
84 ([http://img.jgi.doe.gov/w/doc/about\\_index.html](http://img.jgi.doe.gov/w/doc/about_index.html)). Insertion sequences were detected with IS  
85 Finder (<http://www-is.biotoul.fr/>).

86 **Phylogenetic analyses.** A concatenated gene tree was created using a set of 22 conserved  
87 single-copy phylogenetic marker genes derived from the set used by Ciccarelli et al. (9). The  
88 marker genes were extracted from *E. minutum* and 279 microbial reference genomes  
89 (including "*Endomicrobium*" strain Rs-D17) in the IMG database ver. 2.50 (38), concatenated,  
90 and aligned with MUSCLE (11). The alignment and sequence-associated data (e.g., organism  
91 name) were then imported into ARB (33) and manually refined. A mask was created using the  
92 base frequency filter tool (20% minimal identity) to remove regions of ambiguous positional  
93 homology, yielding a masked alignment of 3982 amino acids, which is available on request  
94 from the authors. Several combinations of outgroups to the TG1 taxa (*E. minutum* and  
95 "*Endomicrobium*" strain Rs-D17) were selected for phylogenetic inference to establish the  
96 monophyly of the TG1 phylum and to identify any specific associations with other phyla that  
97 may exist (10). Maximum-likelihood trees were constructed from the masked datasets using  
98 RAxML ver. HPC-2.2.3 (53).

99 The phylogenetic relationships of the [NiFe] hydrogenase were determined using the ARB  
100 program suite (33). The sequences of *E. minutum* and *Thermoanaerobacter tengcongensis*  
101 were aligned with the sequences of the large subunit given in Vignais et al. (57). Highly  
102 variable positions (< 20% sequence similarity) were filtered from the data set, resulting in 560  
103 unambiguously aligned amino acids, and phylogenetic distances were calculated using the  
104 Protein maximum-likelihood algorithm provided in the ARB package.

105 Clustered, regularly interspaced short palindromic repeats (CRISPR) arrays were identified  
106 using PILER-CR (12). Prophages or other elements targeted by CRISPRs were identified by  
107 pair-wise comparison of spacers to the rest of the genome using BLASTN (2).

## Results and Discussion

108 **Genome structure.** *E. minutum* has a relatively small circular chromosome of 1,643,562 bp  
109 (Fig. 1), with an average G+C content of 39.0 mol%. No plasmids were found. The genome  
110 contains 1597 predicted genes, of which 1529 (95.7%) code for proteins, 48 (3.1%) code for  
111 RNA genes, and 20 (1.3%) are pseudogenes. Of the protein-coding genes, 1141 (74.6%) were  
112 assigned to specific domains in the COG database, and 388 (25.4%) are predicted to be novel  
113 (Table 1). The genome contains only a single rRNA operon, which is in agreement with the  
114 long doubling time of the organism (11–20 h; 14). The G+C content of the rRNA genes  
115 deviates from that of the rest of the genome, which is typical for mesophilic bacteria (40).  
116 There are 45 genes encoding tRNAs for the 20 standard amino acids; tRNA genes with  
117 anticodons for unusual amino acids were not present. The substantial asymmetry in gene  
118 density on the two DNA strands on both sides of the origin indicates the switching between  
119 leading and lagging strands typical of bacteria with a bifurcating replication mechanism (28).

120 The genome contains one array of clustered, regularly interspaced short palindromic repeats  
121 (CRISPR) comprising 13 repeat/spacer units, flanked by an operon containing CRISPR-  
122 associated genes; this region is characterized by a lower G+C content (Fig. 1). CRISPR  
123 elements are widespread in the genomes of almost all archaea and many bacteria and are  
124 considered one of the most ancient antiviral defense systems in the microbial world (37, 52).  
125 One of the *E. minutum* spacers had an identical match within the genome, highlighting the  
126 location of an intact 34-kb prophage. The detailed annotation of all protein-coding genes and  
127 their COG assignments is presented in the supplementary material (Table S1). We detected 63  
128 putative insertion sequences (IS) in the genome, but most of them had only low similarities to  
129 sequences from known IS families (Table S2).



130 **Phylogeny and taxonomy.** As expected for the first cultivated representative of a candidate  
131 phylum, many genes from the *E. minutum* genome are only distantly related to homologs  
132 identified in genomes from other bacterial phyla. The recent publication of a composite  
133 genome of "*Endomicrobium*" strain Rs-D17, recovered from a homogeneous population of  
134 endosymbionts isolated from a single protist cell in a termite hindgut (22), provides a  
135 phylogenetic reference point for analysis. A comparative analysis of 22 concatenated single-  
136 copy marker genes confirmed a highly reproducible relationship between *E. minutum* and  
137 "*Endomicrobium*" strain Rs-D17 (Fig. 2), as predicted already by 16S rRNA-based phylogeny  
138 (20). The analysis also reinforced the phylum-level status proposed for the *Elusimicrobia*  
139 lineage (formerly TG1; 23) since no robust associations to other bacterial phyla were  
140 identified.

141 **Energy metabolism.** Pure cultures of *E. minutum* convert sugars to H<sub>2</sub>, CO<sub>2</sub>, ethanol, and  
142 acetate as major fermentation products (14). A full reconstruction of the energy metabolism by  
143 manual genome annotation (Table S1) revealed that *E. minutum* uses a set of pathways typical  
144 of many strictly fermentative organisms (Fig. 3, blue box). Hexoses are imported via several  
145 phosphotransferase systems (PTS) or permeases. PTS systems for fructose, glucose, and *N*-  
146 acetylglucosamine, three of the five substrates supporting growth of *Elusimicrobium minutum*  
147 (14), were present. The resulting sugar phosphates are converted to fructose 6-phosphate and  
148 degraded to pyruvate via the classical Embden-Meyerhof pathway (EMP); 2-dehydro-3-  
149 deoxy-phosphogluconate aldolase, the key enzyme of the Entner-Doudoroff pathway, is  
150 absent.

151 Pyruvate is further oxidized to acetyl-CoA by pyruvate:ferredoxin oxidoreductase (PFOR).  
152 The acetyl-CoA is converted to acetate by phosphotransacetylase and acetate kinase. There are

153 two enzymes potentially involved in hydrogen formation: a membrane-bound [NiFe]  
154 hydrogenase and a soluble [FeFe] hydrogenase. The [NiFe] hydrogenase operon comprises the  
155 genes encoding the typical subunits; the large subunit contains the two conserved CxxC  
156 motifs found in complex-I-related [NiFe] hydrogenases, and the small subunit has the typical  
157 CxxCx<sub>n</sub>GxCxxxGx<sub>m</sub>GCPP (*E. minutum*:  $n = 61$ ,  $m = 24$ ) motif (1). There is also an operon of  
158 five genes with high similarity to maturation proteins required for the synthesis of the catalytic  
159 metallocluster of [NiFe] hydrogenases (25). Comparative analysis of the genes coding for the  
160 large subunit (*echD*) revealed that the enzyme belongs to group IV [NiFe] hydrogenases (Fig.  
161 4). Hydrogenases of this group function as redox-driven ion pumps, coupling the reduction of  
162 protons by ferredoxin with the generation of a proton-motive force (44, 50), suggesting that  
163 this type of energy conservation may be present also in *E. minutum* (Fig. 3).

164 The second hydrogenase shows the typical structure and sequence motifs of a cytosolic  
165 NADH-dependent [FeFe] hydrogenase (Fig. 5; 51), including the typical H-cluster motif (57).  
166 Since the reduction of NADH to hydrogen is thermodynamically favorable only at low  
167 hydrogen partial pressure (46), this enzyme is probably not involved in hydrogen formation in  
168 batch culture, where hydrogen accumulates to substantial concentrations (14). Here, the  
169 stoichiometry of less than 2 H<sub>2</sub> per glucose indicates that H<sub>2</sub> is formed only via the ferredoxin-  
170 driven [NiFe] hydrogenase; the NADH formed during glycolysis is regenerated by the  
171 reduction of acetyl-CoA to ethanol (Fig. 3).

172 Although it remains to be shown whether *E. minutum* shifts from ethanol to H<sub>2</sub> formation at  
173 low hydrogen partial pressures to increase its energy yield, the presence of the second  
174 hydrogenase may be an adaptation to the low hydrogen partial pressures in its habitat.  
175 Hydrogen concentrations in the hindgut of *Pachnoda ehippiata* were typically below the

176 detection limit of the hydrogen microsensor (60–70 Pa) (30), which is close to the threshold  
177 concentration (< 10 Pa) permitting H<sub>2</sub> formation from NADH (46).

178 **Anabolism.** Although the presence of fructose 1,6-bisphosphatase indicates the possibility for  
179 gluconeogenesis via the EMP, *E. minutum* requires a hexose for growth (14). The absence of  
180 genes coding for 2-oxoglutarate dehydrogenase, succinate dehydrogenase, and succinyl-CoA  
181 synthetase is typical for strict anaerobes and documents that *E. minutum* does not possess a  
182 complete tricarboxylic acid (TCA) cycle. The reductive branch of the incomplete TCA cycle  
183 is initiated by phosphoenol pyruvate (PEP) carboxykinase and allows the interconversion of  
184 oxaloacetate, malate, and fumarate. The oxidative branch of the pathway starts with citrate  
185 synthase and allows the formation of 2-oxoglutarate. Typical for anaerobic microorganisms,  
186 the citrate synthase of *E. minutum* belongs to the *Re*-type (32). The products of the incomplete  
187 TCA cycle are precursors of several amino acids. The biosynthetic pathways for the formation  
188 of glutamate, glutamine, proline, aspartate, lysine, threonine, and cystathione are present. Also  
189 the pathways for the formation of alanine, cysteine, glycine, histidine, and serine, starting with  
190 intermediates of the EMP, are almost fully represented by the corresponding genes (Table S1,  
191 Fig. S1). However, the genes for the synthesis of other proteinogenic amino acids (arginine,  
192 asparagine, isoleucine, leucine, methionine, phenylalanine, tyrosine, tryptophan, and valine)  
193 are lacking, which would explain why *E. minutum* requires small amounts of yeast extract in  
194 the medium (14).

195 The genome of *E. minutum* does not possess an oxidative pentose phosphate pathway, which  
196 is typically involved in the regeneration of NADPH. This important coenzyme is probably  
197 regenerated by the alternative route of pyruvate formation from PEP (formation of  
198 oxaloacetate by PEP carboxykinase, NADH-dependent reduction of oxaloacetate by malate

199 dehydrogenase, and NADP<sup>+</sup>-dependent oxidative decarboxylation of malate by malic enzyme;  
200 Fig. 3, green box), as proposed for *Corynebacterium glutamicum* (45). NADP<sup>+</sup> is required for  
201 the *de novo* biosynthesis of nucleic acids. The presence of the genes required for the non-  
202 oxidative pentose phosphate pathway (transaldolase and transketolase) allows the  
203 reconstruction of the pathways for purine and pyrimidine nucleotide biosynthesis almost  
204 completely (Table S1) and also explains the catabolism of ribose via the EMP (14).

205 Also the genes coding for the synthesis of lipopolysaccharides and peptidoglycan are well  
206 represented (Table S1). This is in agreement with the results of electron microscopy, which  
207 showed that *E. minutum* possesses the typical cell envelope architecture of gram-negative  
208 bacteria (14). The pathways for vitamin synthesis are absent or at most rudimentary (Table  
209 S1), which would be another reason why the bacterium requires small amounts of yeast  
210 extract in the growth medium (14).

211 A large open reading frame (3008 amino acids) was assigned to the polyketide synthase gene  
212 family. Interestingly, the polyketide synthase gene shows a relatively high G+C content (46%;  
213 Fig. 1), suggesting an origin from horizontal gene transfer. The presence of a polyketide  
214 synthase and a putative non-ribosomal peptide synthetase (1284 amino acids) is rather unusual  
215 for anaerobic bacteria (48). The function of the two enzymes remains to be investigated.

216 **Peptide degradation.** *E. minutum* has a particular pathway for catabolic utilization of amino  
217 acids, which may lead to additional energy conservation (Fig. 3, yellow box). The pathway  
218 comprises the transfer of amino groups from peptide-derived amino acids to pyruvate via a  
219 homolog of a non-specific aminotransferase (58), resulting in alanine formation. The 2-  
220 oxoacids produced by the transamination can be oxidatively decarboxylated to the  
221 corresponding acyl-CoA esters, probably by the gene products annotated as 2-

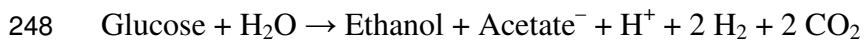
222 oxoacid:ferredoxin oxidoreductases. Substrate-level phosphorylation is accomplished via an  
223 acyl-CoA synthetase (ADP-forming), resulting in the formation of ATP and the corresponding  
224 fatty acid. The genome also encodes proton-dependent oligopeptide transporters, ABC-type  
225 transport systems for peptides, and numerous proteolytic and peptolytic enzymes, some of  
226 which have typical signal peptides, indicating extracellular proteinase activity (Table S1).

227 A comparable peptide utilization pathway is also present in *Pyrococcus furiosus* (34, 36, 19).

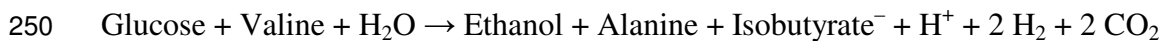
228 Besides the PFOR, a homodimer that typically oxidizes only pyruvate and a few other  
229 oxoacids, e.g., 2-oxoglutarate (39), *E. minutum* also possesses a homologue of a  
230 heterotetrameric 2-oxoisovalerate:ferredoxin oxidoreductase (VFOR) with a broad substrate  
231 specificity, especially for branched-chain 2-oxoacids (19). In addition, a putative two-subunit  
232 indolepyruvate:ferredoxin oxidoreductase (IFOR) is present. The large number of different  
233 acyl-CoA esters resulting from the oxidative decarboxylation of various amino acids seem to  
234 be converted to their corresponding acids by a single ADP-dependent acetyl-CoA synthetase;  
235 the homolog in *P. furiosus* is reportedly rather unspecific and processes also branched-chain  
236 derivatives (35).

237 The operation of this peptide utilization pathway in *E. minutum* is supported by the  
238 observation that most proteinogenic (and even some non-proteinogenic) amino acids are  
239 converted to their corresponding oxidative decarboxylation products during growth on  
240 glucose. Further evidence was provided by <sup>13</sup>C-labeling, which demonstrated that the carbon  
241 skeleton of the putative transamination product, alanine, is derived from glucose (14). In  
242 principle, *E. minutum* also possesses the capacity for the net amination of pyruvate to alanine  
243 (Fig. 3, green box), which has been proposed to function as an additional electron sink in *P.*  
244 *furiosus* (26).

245 A combination of glucose fermentation with the oxidative decarboxylation of an amino acid  
246 can increase the free-energy change of the metabolism, as exemplified by the case of valine  
247 ( $\Delta G^{\circ'}$  values calculated according to 56; data for isobutyrate from 60).



249  $\Delta G^{\circ'} = -225 \text{ kJ mol}^{-1}$



251  $\Delta G^{\circ'} = -245 \text{ kJ mol}^{-1}$

252 However, since substrate-level phosphorylation in the peptide utilization pathway occurs at  
253 the expense of ATP generation from carbohydrates (i.e., pyruvate oxidation), the co-  
254 fermentation of amino acids becomes energetically productive only if this opens up the  
255 possibility for additional energy conservation. Interestingly, *E. minutum* possesses a  
256  $\text{Na}^+$ /alanine symporter, which could couple export of the accumulating alanine with the  
257 generation of an electrochemical sodium gradient. Together with the  $\text{H}^+$ / $\text{Na}^+$  antiporter  
258 encoded in the genome, the sodium gradient can be converted into a proton-motive force,  
259 which would either drive the generation of additional ATP via ATP synthase or avoid the  
260 hydrolysis of ATP necessitated by the dissipation of the proton motive force in other transport  
261 processes (27), such as the proton-dependent import of amino acids or oligopeptides (Fig. 3).

262 **Secretion.** A large number of proteins (40%) encoded in the genome of *E. minutum* contain a  
263 signal peptide, indicating their export from the cell (Table S1). These putatively exported  
264 proteins comprise almost all of the proteins in COG category U (intracellular trafficking,  
265 secretion, and vesicular transport) and more than half of the predicted novel proteins.

266 The results of the manual annotation revealed that *E. minutum* possesses a variant of the  
267 general secretion pathway (GSP). The Sec translocon (encoded by *secADFYEG*) lacks a SecB  
268 subunit; SecB is probably replaced by one of the more general chaperones (DnaJ or DnaK)  
269 (59). There are numerous genes encoding the typical type II secretion system (T2SS), but  
270 several essential components of the machinery are missing in the annotation (Table 2). Most  
271 of these components are poorly conserved (encoded by *gspABCNS*; 8) and might have simply  
272 escaped detection. Some of the missing elements might have been annotated as elements of  
273 type IV pili (T4P), which are related structures with numerous similar components (55). T4P  
274 are probably absent in *E. minutum* because the PilMNOP components, which are essential for  
275 functional pili (6, 5), are lacking and no pilus-like structures are seen in ultra-thin sections of  
276 *E. minutum* (14). The absence of *gspL* and *gspM* in *E. minutum* is more critical because the  
277 encoded proteins have no homologs in T4P and are usually indicative of a T2SS. However,  
278 also the T2SS of *Acinetobacter calcoaceticus* and *Bdellovibrio bacteriovorus* lack the GspLM  
279 components (8), and the pathogen *Francisella tularensis* ssp. *novicidia* uses a T2SS even  
280 lacking the GspLMC components to export chitinases, proteinases, and  $\beta$ -glucosidases (16).  
281 The presence of two ATPases in *E. minutum*, which are typical for T4P, does not necessarily  
282 argue against a T2SS; the T2SS of *Aeromonas hydrophila* also has two ATPases, and they are  
283 thought to increase the efficiency of the secretory process (47).

284 The number of *pilE*-like genes in the genome of *E. minutum* is much higher than the number  
285 of all other components of the T2SS. Sixty *pilE*-like genes (members of COG4968) are spread  
286 over the genome (Table S1). It has been shown that variable gene copies of *pilE* play a role in  
287 immune evasion because they lead to antigenic variations in the pilins of the *Neisseria*  
288 *gonorrhoeae* T4P (17). Although the pilins of T2SS reach through the periplasm and the outer  
289 membrane, their importance as an antigen is not clear. It is also not clear whether antigenic

290 variation is important for the colonization of the insect gut. Although insects lack an adaptive  
291 immune system with antigen-specific antibodies, it has been reported that a response to an  
292 immune challenge can be enhanced by previous exposure (29).

293 Comparative analysis revealed that only the encoded N-terminal methylase domain is  
294 conserved between the *E. minutum pilE*-like genes and *pilE* genes from other organisms. This  
295 effectively reduces the comparable region to only ~50 amino acids and compromises  
296 phylogenetic inference. However, it appears that most of the *E. minutum* copies (57/60) form a  
297 monophyletic group, which suggests a large lineage-specific expansion of this gene family, or  
298 at least an expansion of the gene domain (data not shown). Indeed, the numerous copies of the  
299 *pilE*-like genes of the *E. minutum* genome alone increase the size of the COG4968 family in  
300 the IMG database by almost 10% because there are only 682 representatives present in 1087  
301 other microbial genomes (38). Since *E. minutum* lacks observable pili and many of the *pilE*-  
302 like genes appear in operons of diverse function, we speculate that this gene family is  
303 involved in some other aspect(s) of endogenous regulation, perhaps not related to pili or  
304 secretion at all, and have undergone a lineage-specific expansion in response to environmental  
305 selection.

306 In addition to the type-II-like secretion system, the genome contains numerous ABC  
307 transporters (Table S1). Together with outer membrane efflux proteins (OMP, MFP), they  
308 may constitute type I secretion systems with various functions.

309 **Oxygen stress.** In agreement with the obligately anaerobic nature of *E. minutum*, the genome  
310 contains no cytochrome genes and no pathways for the biosynthesis of quinones,  
311 corroborating the absence of any respiratory electron transport chains. However, *E. minutum*  
312 has a six-gene "oxygen stress protection" cluster consisting of ruberythrin (*rbr*), superoxide



313 reductase (*sor*), rubredoxin:oxygen oxidoreductase (*roo*), and rubredoxin (*rub*) (Fig. 6). The  
314 *roo* gene of *E. minutum* has similarity to the corresponding genes of *Desulfovibrio gigas* and  
315 *Moorella thermoacetica*, which have been shown to reduce molecular oxygen by reduced  
316 rubredoxin (15, 49). The presence of an oxygen-reducing system may explain the ability of *E.*  
317 *minutum* to retard the diffusive influx of oxygen into deep-agar tubes (14) and may play an  
318 important role in survival in the intestinal tract of insects, a habitat constantly exposed to the  
319 influx of oxygen (4, 31).

320 **Ecological considerations.** The genome of *E. minutum* revealed several adaptations of the  
321 bacterium to its environment. As a member of the "Intestinal Cluster", *E. minutum* is probably  
322 a resident inhabitant of the gut of *P. ehippiata*, which is thought to assist in digestion (31). *P.*  
323 *ehippiata* feeds on a humus-rich diet, and its gut contains high concentrations of glucose,  
324 peptides, and amino acids (3). With its putative capacity for proteinase secretion, the potential  
325 to maximize ATP yield in a coupled fermentation of sugars and amino acids, and the ability to  
326 cope with the exposure to molecular oxygen and reactive oxygen species, *E. minutum* appears  
327 to be well adapted to this habitat. As with other intestinal bacteria, it requires complex  
328 nutritive supplements and lacks pathways for the synthesis of most vitamins and certain amino  
329 acids. Although the genome of *E. minutum* is relatively small, there are no indications for an  
330 obligate association with its host. Genes encoding glycosyl hydrolases involved in the  
331 degradation of polysaccharides (other than glycogen) were not identified, indicating that *E.*  
332 *minutum* does not participate in the digestion of plant fibers.

## Acknowledgements

333 We thank members of the JGI production sequencing, quality assurance and genome biology  
334 programs and the IMG team for their assistance in genome sequencing, assembly, annotation,  
335 and loading of the genome into IMG. These activities were supported by the 2007 Community  
336 Sequencing Program. D.H. and W.I.-O. were supported by stipends of the International Max  
337 Planck Research School for Molecular, Cellular, and Environmental Microbiology and the  
338 Deutscher Akademischer Austauschdienst. We thank Henning Seedorf, Reiner Hedderich, and  
339 Rolf Thauer (Marburg) for helpful advice. This work was financed in part by a grant of the  
340 Deutsche Forschungsgemeinschaft (DFG) in the Collaborative Research Center Transregio 1  
341 (SFB-TR1) and by the Max Planck Society. Other parts of this work were performed under  
342 the auspices of the US Department of Energy's Office of Science, Biological and  
343 Environmental Research Program, and by the University of California, Lawrence Berkeley  
344 National Laboratory under contract No. DE-AC02-05CH11231, Lawrence Livermore  
345 National Laboratory under Contract No. DE-AC52-07NA27344, and Los Alamos National  
346 Laboratory under contract No. DE-AC02-06NA25396.

## References

- 347 1. **Albracht, S. P. J.** 1994. Nickel hydrogenases: in search of the active site. *Biochim.*  
348 *Biophys. Acta* **1188**: 167–204.
- 349 2. **Altschul, S. F., T. L. Madden, A. A. Schäffer, J. Zhang, Z. Zhang, W. Miller, and**  
350 **D. J. Lipman.** 1997. Gapped BLAST and PSI-BLAST: a new generation of protein  
351 database search programs. *Nucleic Acids Res.* **25**: 3389–3402.
- 352 3. **Andert, J., O. Geissinger, and A. Brune.** 2008. Peptidic soil components are a major  
353 dietary resource for the humivorous larvae of *Pachnoda* spp. (Coleoptera:  
354 Scarabaeidae). *J. Ins. Physiol.* **54**: 105–113.
- 355 4. **Brune, A., P. Frenzel, and H. Cypionka.** 2000. Life at the oxic-anoxic interface:  
356 microbial activities and adaptations. *FEMS Microbiol. Rev.* **24**: 691–710.
- 357 5. **Carbonnelle, E., S. Hélaïne, L. Prouvensier, X. Nassif, and V. Pelicic.** 2005. Type IV  
358 pilus biogenesis in *Neisseria meningitidis*: PilW is involved in a step occurring after  
359 pilus assembly, essential for fibre stability and function. *Mol. Microbiol.* **55**: 54–64.
- 360 6. **Carbonnelle, E., S. Hélaïne, X. Nassif, and V. Pelicic.** 2006. A systematic genetic  
361 analysis in *Neisseria meningitidis* defines the Pil proteins required for assembly,  
362 functionality, stabilization and export of type IV pili. *Mol. Microbiol.* **61**: 1510–1522.
- 363 7. **Caspi, R., H. Foerster, C. A. Fulcher, R. Hopkinson, J. Ingraham, P. Kaipa, M.**  
364 **Krummenacker, S. Paley, J. Pick, S. Y. Rhee, C. Tissier, P. Zhang, and P. D. Karp.**  
365 2006. MetaCyc: a multiorganism database of metabolic pathways and enzymes. *Nucleic*  
366 *Acids Res.* **34**: D511–516.

- 367 **8. Cianciotto, N. P.** 2005. Type II secretion: a protein secretion system for all seasons.  
368 *Trends Microbiol.* **13**: 281–288.
- 369 **9. Ciccarelli, F. D., T. Doerks, C. von Mering, C. J. Creevey, B. Snel, and P. Bork.**  
370 2006. Toward automatic reconstruction of a highly resolved tree of life. *Science* **311**:  
371 1283–1287.
- 372 **10. Dalevi, D., P. Hugenholtz, and L. L. Blackall.** 2001. A multiple-outgroup approach to  
373 resolving division-level phylogenetic relationships using 16S rDNA data. *Int. J. Syst.*  
374 *Evol. Microbiol.* **51**: 385–391.
- 375 **11. Edgar, R. C.** 2004. MUSCLE: multiple sequence alignment with high accuracy and  
376 high throughput. *Nucleic Acids Res.* **32**: 1792–1797.
- 377 **12. Edgar, R. C.** 2007. PILER-CR: Fast and accurate identification of CRISPR repeats.  
378 *Bioinformatics* **8**: 18
- 379 **13. Filloux, A.** 2004. The underlying mechanism of type II protein secretion. *Biochim.*  
380 *Biophys. Acta* **1694**: 163–179.
- 381 **14. Geissinger, O., D. P. R. Herlemann, U. G. Maier, E. Mörschel, and A. Brune.**  
382 *Elusimicrobium minutum* gen. nov., sp. nov., the first isolate of the Termite Group I  
383 phylum (submitted).
- 384 **15. Gomes, C. M., G. Silva, S. Oliveira, J. LeGall, M.-Y. Liu, A. V. Xavier, C.**  
385 **Rodrigues-Pousada, and M. Teixeira.** 1997. Studies on the redox centers of the  
386 terminal oxidase from *Desulfovibrio gigas* and evidence for its interaction with  
387 rubredoxin. *J. Biol. Chem.* **272**: 22502–22508.

- 388 **16. Hager, A. J., D. L. Bolton, M. R. Pelletier, M. J. Brittnacher, L. A. Gallagher, R.**  
389 **Kaul, J. S. Skerrett, I. S. Miller, and T. Gulna.** 2006. Type IV pili-mediated secretion  
390 modulates *Francisella* virulence. *Mol. Microbiol.* **62**: 227–237.
- 391 **17. Häggblom, P., E. Segal, E. Billyard, and M. So.** 1985. Intragenic recombination leads  
392 to pilus antigenic variation in *Neisseria gonorrhoeae*. *Nature* **315**: 156–158.
- 393 **18. Hauser, L., F. Larimer, M. Land, M. Shah, and E. Uberbacher.** 2004. Analysis and  
394 annotation of microbial genome sequences, p. 225–238. In Setlow J. K. (ed), *Genetic*  
395 *Engineering*, Vol. 26. Kluwer Academic, New York, NY.
- 396 **19. Heider, J., X. Mai, and M. W. Adams.** 1996. Characterization of 2-ketoisovalerate  
397 ferredoxin oxidoreductase, a new and reversible coenzyme A-dependent enzyme  
398 involved in peptide fermentation by hyperthermophilic archaea. *J. Bacteriol.* **178**: 780–  
399 787.
- 400 **20. Herlemann, D. P. R., O. Geissinger, and A. Brune.** 2007. The Termite Group I  
401 phylum is highly diverse and widespread in the environment. *Appl. Environ. Microbiol.*  
402 **73**: 6682–6685.
- 403 **21. Hongoh, Y., M. Ohkuma, and T. Kudo.** 2003. Molecular analysis of bacterial  
404 microbiota in the gut of the termite *Reticulitermes speratus* (Isoptera, Rhinotermitidae).  
405 *FEMS Microbiol Ecol.* **44**: 231–242.
- 406 **22. Hongoh, Y., V. K. Sharma, T. Prakash, S. Noda, T. D. Taylor, T. Kudo, Y. Sakaki,**  
407 **A. Toyoda, M. Hattori, and M. Ohkuma.** 2008. Complete genome of the uncultured  
408 Termite Group 1 bacteria in a single host protist cell. *Proc. Natl. Acad. Sci. U.S.A.* **105**:  
409 5555–5560.

- 410 **23. Hugenholtz, P., B. M. Goebel, and N. R. Pace.** 1998. Impact of culture-independent  
411 studies on the emerging phylogenetic view of bacterial diversity. *J Bacteriol.* **180**:  
412 4765–4774.
- 413 **24. Ikeda-Ohtsubo, W., M. Desai, U. Stingl, and A. Brune.** 2007. Phylogenetic diversity  
414 of "Endomicrobia" and their specific affiliation with termite gut flagellates.  
415 *Microbiology* **153**: 3458–3465.
- 416 **25. Jacobi A., R. Rossmann, and A. Böck.** 1992. The *hyp* operon gene products are  
417 required for the maturation of catalytically active hydrogenase isoenzymes in  
418 *Escherichia coli*. *Arch. Microbiol.* **158**: 444–451.
- 419 **26. Kengen, S. W. M., and A. J. M. Stams.** 1994. Formation of l-alanine as a reduced end  
420 product in carbohydrate fermentation by the hyperthermophilic archaeon *Pyrococcus*  
421 *furius*. *Arch. Microbiol.* **161**: 168–175.
- 422 **27. Konings W.N.** 2006. Microbial transport: adaptations to natural environments. *Antonie v.*  
423 *Leeuwenhoek* **90**: 325–42.
- 424 **28. Koonin E.V. and Y.I. Wolf.** 2008. Genomics of bacteria and archaea: the emerging  
425 dynamic view of the prokaryotic world. *Nucleic Acids Res.* **36**: 6688–719.
- 426 **29. Kurtz, J.** 2004. Memory in the innate and adaptive immune systems. *Microbes and*  
427 *Infection* **6**: 1410–1417.
- 428 **30. Lemke T., T. van Alen, J. H. P. Hackstein, and A. Brune.** 2001. Cross-epithelial  
429 hydrogen transfer from the midgut compartment drives methanogenesis in the hindgut  
430 of cockroaches. *Appl. Environ. Microbiol.* **67**: 4657–4661. Tables

- 431 **31. Lemke, T., U. Stingl, M. Egert, M. W. Friedrich, and A. Brune.** (2003)  
432 Physicochemical conditions and microbial activities in the highly alkaline gut of the  
433 humus-feeding larva of *Pachnoda ephippiata* (Coleoptera: Scarabaeidae). *Appl.*  
434 *Environ. Microbiol.* **69**: 6650–6658.
- 435 **32. Li, F., C. H. Hagemeyer, H. Seedorf, G. Gottschalk, and R. K. Thauer.** 2007. *Re-*  
436 *citrate synthase from *Clostridium kluyveri* is phylogenetically related to homocitrate*  
437 *synthase and isopropylmalate synthase rather than to Si-citrate synthase. J. Bacteriol.*  
438 **189**: 4299–304.
- 439 **33. Ludwig, W., O. Strunk, R. Westram, L. Richter, H. Meier, Yadhukumar, A.**  
440 **Buchner, T. Lai, S. Steppi, G. Jobb, W. Förster, I. Brettske, S. Gerber, A. W.**  
441 **Ginhart, O. Gross, S. Grumann, S. Hermann, R. Jost, A. König, T. Liss, R.**  
442 **Lüßmann, M. May, B. Nonhoff, B. Reichel, R. Strehlow, A. Stamatakis, N.**  
443 **Stuckmann, A. Vilbig, M. Lenke, T. Ludwig, A. Bode, and K.-H. Schleifer.** 2004.  
444 *ARB: a software environment for sequence data. Nucleic Acids Res.* **32**: 1363–1371.
- 445 **34. Mai, X., and M. W. W. Adams.** 1994. Indolepyruvate ferredoxin oxidoreductase from  
446 the hyperthermophilic archaeon *Pyrococcus furiosus*. A new enzyme involved in  
447 peptide fermentation. *J. Biol. Chem.* **269**: 16726–32.
- 448 **35. Mai, X., and M. W. W. Adams.** 1996a. Characterization of a fourth type of 2-keto  
449 acid-oxidizing enzyme from a hyperthermophilic archaeon: 2-ketoglutarate ferredoxin  
450 oxidoreductase from *Thermococcus litoralis*. *J. Bacteriol.* **178**: 5890–5896.

- 451 **36. Mai, X., and M. W. W. Adams.** 1996b. Purification and characterization of two  
452 reversible and ADP-dependent acetyl coenzyme A synthetases from the  
453 hyperthermophilic archaeon *Pyrococcus furiosus*. *J. Bacteriol.* **178**: 5897–5903.
- 454 **37. Makarova, K. S., N. V. Grishin, S. A. Shabalina, J. I. Wolf, and V. K. Eugene.**  
455 2006. A putative RNA-interference-based immune system in prokaryotes:  
456 computational analysis of the predicted enzymatic machinery, functional analogies with  
457 eukaryotic RNAi, and hypothetical mechanisms of action. *Biol. Direct.* **1**: 7.
- 458 **38. Markowitz, V. M., E. Szeto, K. Palaniappan, Y. Grechkin, K. Chu, I. M. Chen, I.**  
459 **Dubchak, I. Anderson, A. Lykidis, K. Mavromatis, N. N. Ivanova, and N. C.**  
460 **Kyrpides.** 2008. The integrated microbial genomes (IMG) system in 2007: data content  
461 and analysis tool extensions. *Nucleic Acids Res.* **36**: D528–D533.
- 462 **39. Moulis, J. M., V. Davasse, J. Meyer, and J. Gaillard.** 1996. Molecular mechanism of  
463 pyruvate-ferredoxin oxidoreductases based on data obtained with the *Clostridium*  
464 *pasteurianum* enzyme. *FEBS Lett.* **380**: 287–290.
- 465 **40. Muto, A., and S. Osawa.** 1987. The guanine and cytosine content of genomic DNA and  
466 bacterial evolution. *Proc. Natl. Acad. Sci. U.S.A.* **84**: 166–9.
- 467 **41. Ohkuma, M., and T. Kudo.** 1996. Phylogenetic diversity of the intestinal bacterial  
468 community in the termite *Reticulitermes speratus*. *Appl Environ Microbiol.* **62**: 461–  
469 468.
- 470 **42. Ohkuma, M., T. Sato, S. Noda, S. Ui, T. Kudo, and Y. Hongoh.** 2007. The candidate  
471 phylum 'Termite Group 1' of bacteria: phylogenetic diversity, distribution, and



- 472 endosymbiont members of various gut flagellated protists. *FEMS Microbiol. Ecol.* **60**:  
473 467–476.
- 474 **43. Rappe, M. S., and S. J. Giovannoni.** 2003. The uncultured microbial majority. *Annu.*  
475 *Rev. Microbiol.* **57**: 369–394.
- 476 **44. Sapro, R., K. Bagramyan, and M. W. Adams.** 2003. A simple energy-conserving  
477 system: proton reduction coupled to proton translocation. *Proc. Natl. Acad. Sci. U.S.A.*  
478 **100**: 7545–50.
- 479 **45. Sauer, U., and B. J. Eikmanns.** 2005. The PEP-pyruvate-oxaloacetate node as the  
480 switch point for carbon flux distribution in bacteria. *FEMS Microbiol. Rev.* **29**: 765–  
481 794.
- 482 **46. Schink, B.** 1997. Energetics of syntrophic cooperation in methanogenic degradation.  
483 *Microbiol. Mol. Biol. Rev.* **61**: 262–280.
- 484 **47. Schoenhofen, I. C., G. Li, T. G Strozen, and S. P. Howard.** 2005. Purification and  
485 characterization of the N-terminal domain of ExeA: a novel ATPase involved in the  
486 type II secretion pathway of *Aeromonas hydrophila*. *J. Bacteriol.* **187**: 6370–63708.
- 487 **48. Seedorf, H., W. F. Fricke, B. Veith, H. Brüggemann, H. Liesegang, A. Strittmatter,**  
488 **M. Miethke, , Buckel, W., J. Hinderberger, F. Li, C. Hagemeyer, R. K. Thauer, and**  
489 **G. Gottschalk.** 2008. The genome of *Clostridium kluyveri*, a strict anaerobe with  
490 unique metabolic features. *Proc. Natl. Acad. Sci. U.S.A.* **105**: 2128–2133.
- 491 **49. Silaghi-Dumitrescu, R., E. D. Coulter, A. Das, L. G. Ljungdahl, G. N. Jameson, B.**  
492 **H. Huynh, and D.M. Kurtz, Jr..** 2003. A flavodiiron protein and high molecular

- 493 weight rubredoxin from *Moorella thermoacetica* with nitric oxide reductase activity.  
494 *Biochemistry* **42**: 2806–2815.
- 495 **50. Soboh, B., D. Linder, and R. Hedderich.** 2002. Purification and catalytic properties of  
496 a CO-oxidizing:H<sub>2</sub>-evolving enzyme complex from *Carboxydotherrmus*  
497 *hydrogenoformans*. *Eur. J. Biochem.* **269**: 5712–21.
- 498 **51. Soboh, B., D. Linder, and R. Hedderich.** 2004. A multisubunit membrane-bound  
499 [NiFe] hydrogenase and an NADH-dependent Fe-only hydrogenase in the fermenting  
500 bacterium *Thermoanaerobacter tengcongensis*. *Microbiology* **150**: 2451–2463.
- 501 **52. Sorek, R., Y. Zhu, C. J. Creevey, P. M. Francino, P. Bork, and E. M. Rubin.** 2007.  
502 Genome-wide experimental determination of barriers to horizontal gene transfer.  
503 *Science* **318**: 1449–1452.
- 504 **53. Stamatakis, A.** 2006. RAxML-VI-HPC: maximum likelihood-based phylogenetic  
505 analyses with thousands of taxa and mixed models. *Bioinformatics* **22**: 2688–90.
- 506 **54. Stingl, U., R. Radek, H. Yang, and A. Brune.** 2005. 'Endomicrobia': Cytoplasmic  
507 symbionts of termite gut protozoa form a separate phylum of prokaryotes. *Appl.*  
508 *Environ. Microbiol.* **71**: 1473–1479.
- 509 **55. Strom, M. S., D. Nunn, and S. Lory.** 1991. Multiple roles of the pilus biogenesis  
510 protein PilD: Involvement of the PilD in excretion of enzymes from *Pseudomonas*  
511 *aeruginosa*. *J. Bacteriol.* **173**: 1175–1180.
- 512 **56. Thauer, R. K., K. Jungermann, and K. Decker.** 1977. Energy conservation in  
513 chemotrophic anaerobic bacteria. *Bacteriol. Rev.* **41**: 100–180.

- 514 **57. Vignais, P. M., B. Billoud, and J. Meyer.** 2001. Classification and phylogeny of  
515 hydrogenases. *FEMS Microbiol. Rev.* **25**: 455–501.
- 516 **58. Ward, D. E., S. W. Kengen, J. van der Oost, and W. M. de Vos.** 2000. Purification  
517 and characterization of the alanine aminotransferase from the hyperthermophilic  
518 archaeon *Pyrococcus furiosus* and its role in alanine production. *J. Bacteriol.* **182**:  
519 2559–2566.
- 520 **59. Wild, J., E. Altman, T. Yura, and C. A. Gross.** 1992. DnaK and DnaJ heat shock  
521 proteins participate in protein export in *Escherichia coli*. *Genes Dev.* **6**: 1165–1172.
- 522 **60. Wu, W.-M., M. Jain, K. Hickey, and J. G. Zeikus.** 1996. Perturbation of syntrophic  
523 isobutyrate and butyrate degradation with formate and hydrogen. *Biotechnol. Bioeng.*  
524 **52**: 404–411.

## Tables

525 TABLE 1. Summary of the functional assignment, according to COG domain, of the 1529  
 526 protein-coding genes in the *Elusimicrobium minutum* genome. Details are shown in the  
 527 supplementary material (Table S1).

COG group	Number of genes <sup>a</sup>	Gene frequency (%)	COG function definition
C	67	4	Energy production and conversion
D	19	1	Cell cycle control, cell division, chromosome partitioning
E	83	5	Amino acid transport and metabolism
F	53	3	Nucleotide transport and metabolism
G	73	5	Carbohydrate transport and metabolism
H	42	3	Coenzyme transport and metabolism
I	37	2	Lipid transport and metabolism
J	117	8	Translation, ribosomal structure, and biogenesis
K	46	3	Transcription
L	76	5	Replication, recombination, and repair
M	109	7	Cell wall/membrane/envelope biogenesis
N	84	5	Cell motility
O	45	3	Posttranslational modification, protein turnover, chaperones
P	24	2	Inorganic ion transport and metabolism
Q	10	1	Secondary metabolites biosynthesis, transport, and catabolism
R	123	8	General function prediction only
S	72	5	Function unknown
T	32	2	Signal transduction mechanisms
U	114	7	Intracellular trafficking, secretion, and vesicular transport
V	19	1	Defense mechanisms
–	388	25	Unassigned (predicted to be novel)

528 <sup>a</sup> A number of genes belong to more than one category

1 TABLE 2. Comparison of the components of the type II secretion system (*gsp* genes) and type IV pili (*pil* genes) present in *Aeromonas*  
2 *hydrophila* and *Francisella tularensis* ssp. *novicida* with those of *Elusimicrobium minutum*. The information is based on COG assignment and  
3 was collected from the IMG platform. Homologous structures present in both systems are given in the same row. Bold letters indicate typical  
4 components of the respective system; nomenclature follows that of Filloux (13).

COG	Function	<i>gsp</i>	<i>pil</i>	<i>Aeromonas hydrophila</i> <sup>a,b</sup>	<i>Francisella tularensis</i> <sup>b,c</sup>	<i>Elusimicrobium minutum</i>
4796	Secretin	<b>D</b>	Q	+	+	+
2804	Fimbrial assembly	<b>E</b>	B	+	+	+
1459	Fimbrial assembly	<b>F</b>	C, Y1	+	+	+
4969	Pilin	<b>G</b>	A	+	+	+
1989	Prepilin kinase	<b>O</b>	<b>D</b>	+	+	+
3168	Stabilizing lipoprotein	<b>S</b>	<b>P</b>	+	+	–
4726	Pilin-like	<b>K</b>	X	+	–	–
2165	Minor pilin	<b>H, I, J</b>		+	–	+
3149	Membrane location	<b>M</b>		+	–	–
3031	Unknown	<b>C</b>		+	–	–
3297	Function unknown	<b>L</b>		+	–	–
3267	Unknown	A		+	–	–
3063	Fimbrial assembly		<b>F</b>	+	–	+
4972	Fimbrial biogenesis		<b>M</b>	+	–	+

3156	Fimbrial assembly	N	+	-	-
3176	Fimbrial assembly	O	+	-	-
2805	Twitching motility	T	+	+	+
4968	Pilin-like	E	+	+	+
4966	Pilin-like	W	+	+	-
4970	Pilin-like	U	+	+	-
4967	Pilin-like	V	+	-	-
5008	Twitching motility	U	+	-	-
642	Two-component system	S	+	+	+
745	Chemosensory	H, G	+	+	+
835	Chemosensory	I	+	-	-
840	Chemosensory	J	+	-	+

---

- 1 <sup>a</sup> Organism possesses type IV pili (13)
- 2 <sup>b</sup> Organism possesses a type II secretion system (13, 16)
- 3 <sup>c</sup> The type II secretion system is incomplete and pili-like fibers were not detected (16).

## Figure legends

1 FIG. 1. Genomic organization of the *Elusimicrobium minutum* chromosome. The two  
2 outermost rings show the genes encoded on the forward and reverse strand (scale in  
3 mega base pairs). The third ring depicts the location of tRNA genes. The fourth ring  
4 shows the G+C content and the innermost ring the GC skew. The polyketide synthase  
5 (PKS) and rRNA operons have a relatively high G+C content; a prophage and several  
6 predicted novel genes have a relatively low G+C content. GC skew was used to identify  
7 the origin of replication (Ori).

8 FIG. 2. An unrooted maximum-likelihood tree of 280 bacterial genomes, including the two  
9 sequenced representatives of the phylum *Elusimicrobia*, representing the regions of the  
10 bacterial domain currently mapped by genome sequences. The tree is based on a  
11 concatenated alignment of 22 single-copy genes. Reproducibly monophyletic groups of  
12 taxa (>98% bootstrap values, except for the *Deltaproteobacteria*; 82%) are grouped into  
13 wedges for clarity. The apparent relationship between *Elusimicrobia* and the  
14 *Synergistetes* is not stable.

15 FIG. 3. Schematic overview of the energy metabolism in *Elusimicrobium minutum*. Sugars  
16 are degraded via the Embden-Meyerhof pathway and pyruvate-ferredoxin  
17 oxidoreductase (PFOR) (blue box). NADH is recycled by reduction of acetyl-CoA to  
18 ethanol or, at low hydrogen partial pressure, by the cytoplasmic [FeFe] hydrogenase.  
19 Reduced ferredoxin is regenerated by the membrane-bound [NiFe] hydrogenase. Amino  
20 acids are metabolized by transamination with pyruvate and subsequently oxidatively  
21 decarboxylated to the corresponding acids by several homologs of PFOR (yellow box).  
22 Alanine can be generated not only by transamination but also by reductive amination of

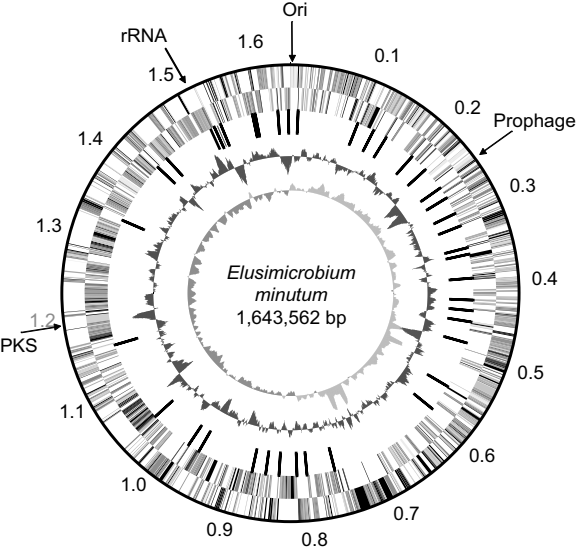
1 pyruvate (green box). The export of alanine generates a sodium-motive force, which is  
2 coupled to the proton-motive force, the synthesis/hydrolysis of ATP via ATP synthase,  
3 and the proton-dependent uptake of amino acids or oligopeptides. Pathways were  
4 reconstructed based on the manually annotated genome and results from batch culture  
5 experiments (16).

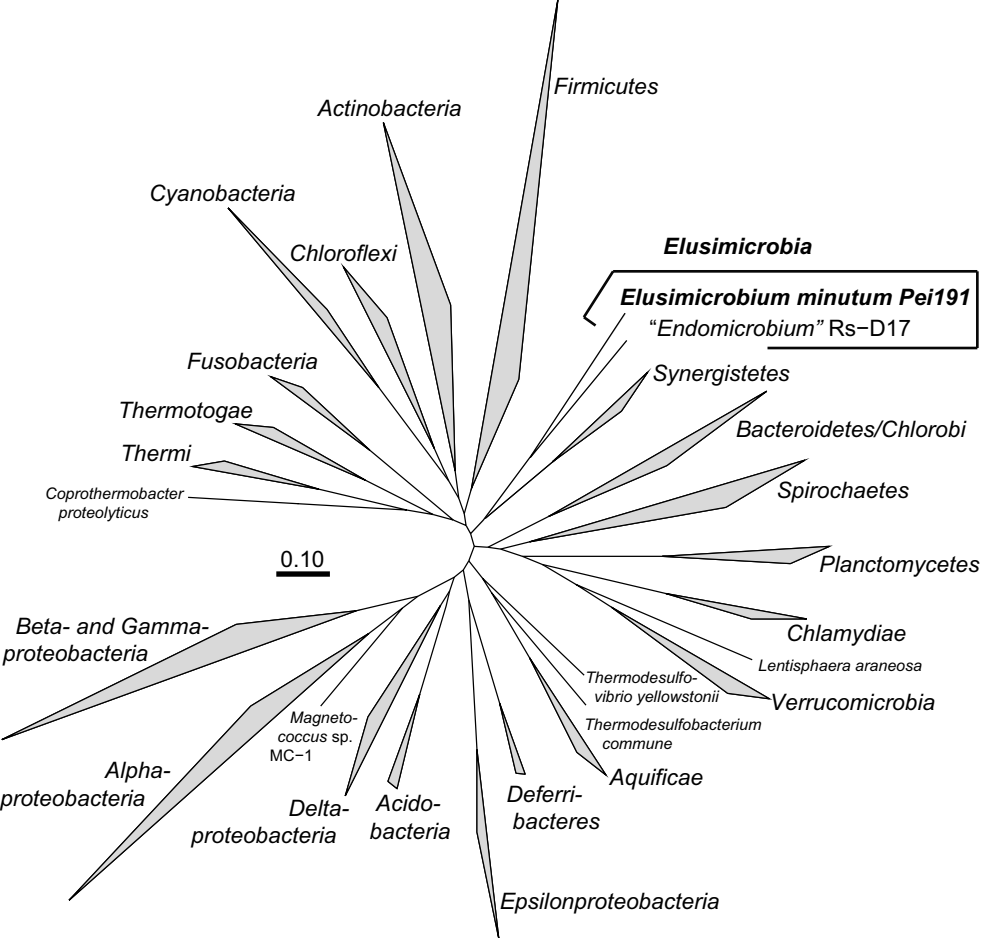
6 FIG. 4. Maximum-likelihood tree of [NiFe] hydrogenases, based deduced amino acid  
7 sequences of the large subunit. The sequences of *Elusimicrobium minutum* and  
8 *Thermoanaerobacter tengcongensis* fall within the radiation of the sequences assigned  
9 to group IV [NiFe] hydrogenases by (54). The topology of the tree was tested separately  
10 by neighbor-joining and RAxML, with bootstrapping provided in the ARB package  
11 (31).

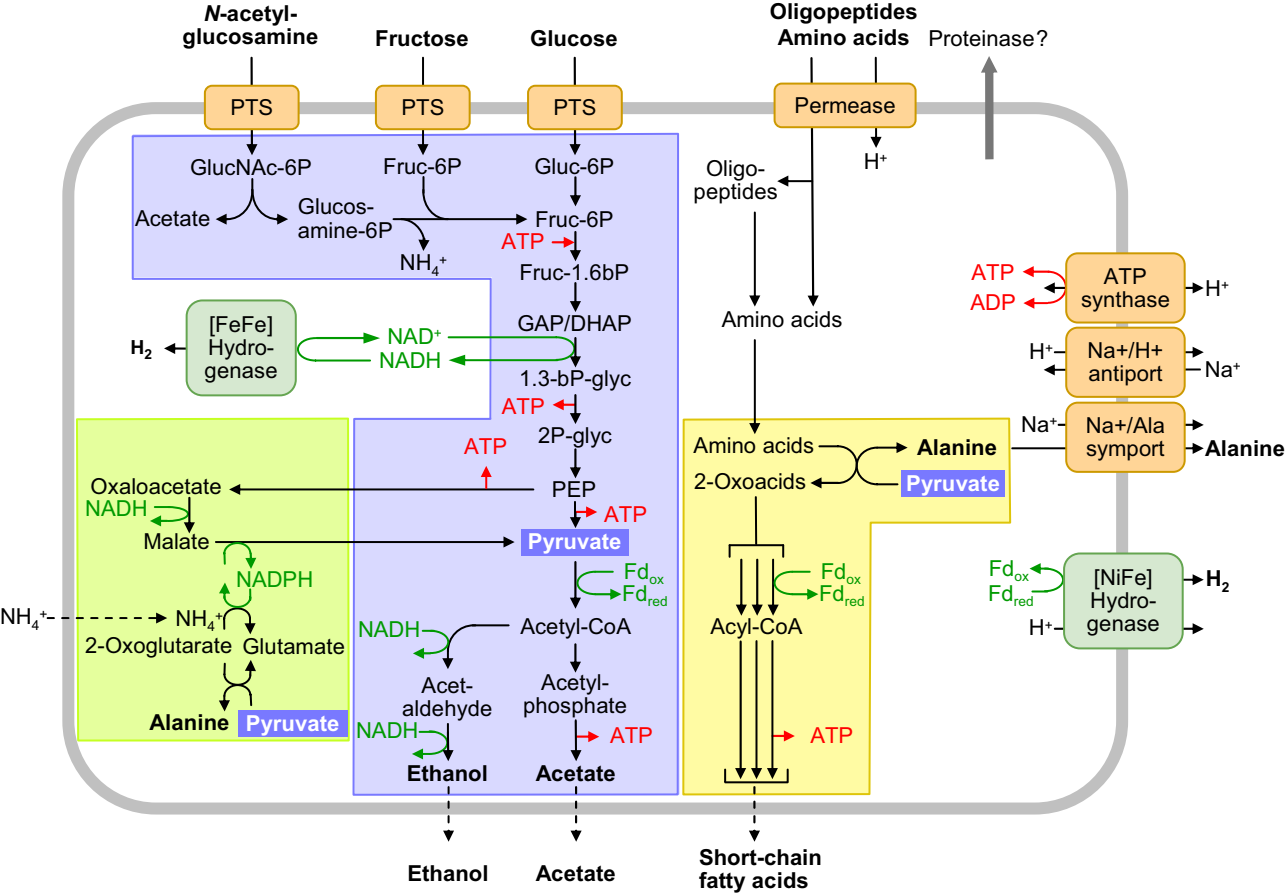
12 FIG. 5. Organization of the genes encoding the subunits of the [FeFe] hydrogenase of *T.*  
13 *tengcongensis* (48) and their predicted homologs in *Elusimicrobium minutum*. The  
14 displayed length is proportional to the size of the corresponding ORF. *hydA*, *hydB*, and  
15 *hydC* have deduced amino acid sequence identities of 46, 56, and 40%, respectively  
16 *hydD* is not present in *E. minutum*. White symbols: hypothetical function.

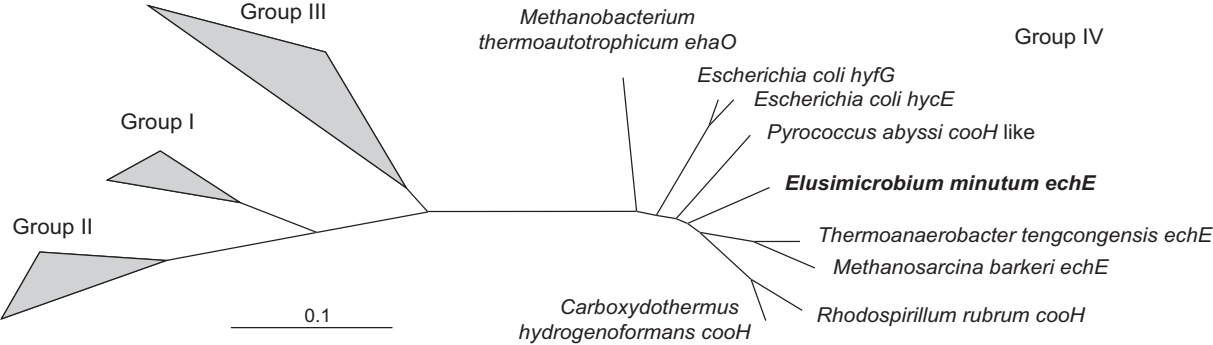
17 FIG. 6. Organization of the genes encoding the "oxidative stress protection" cluster in  
18 *Moorella thermoacetica*, *Desulfovibrio gigas*, and their predicted homologs in  
19 *Elusimicrobium minutum*. The displayed length is proportional to the size of the  
20 corresponding ORF. The genes for ruberythrin (*rbr*), superoxide reductase (*sor*),  
21 rubredoxine:oxygen oxidoreductase (*roo*), rubredoxin (*rub*) and rubredoxin-like (*rbl*) in  
22 *E. minutum* have high sequence similarities to their homologs in *Desulfovibrio* spp. and  
23 other *Deltaproteobacteria*. White symbol: hypothetical function.











*Thermo-  
anaerobacter  
tengcongensis*



*Elusimicrobium  
minutum*



*Elusimicrobium  
minutum*



*Desulfovibrio  
vulgaris*



*Moorella  
thermoacetica*

